

## Long-Living Bloch Oscillations of Matter Waves in Periodic Potentials

M. Salerno,<sup>1</sup> V. V. Konotop,<sup>2,3</sup> and Yu. V. Bludov<sup>3</sup>

<sup>1</sup>*Dipartimento di Fisica E. R. Caianiello, and Consorzio Nazionale Interuniversitario per le Scienze Fisiche della Materia (CNISM), Università di Salerno, I-84081, Baronissi (SA), Italy*

<sup>2</sup>*Departamento de Física, Universidade de Lisboa, Campo Grande, Edifício C8, Piso 6, Lisboa 1749-016, Portugal*

<sup>3</sup>*Centro de Física Teórica e Computacional, Universidade de Lisboa, Complexo Interdisciplinar, Avenida Professor Gama Pinto 2, Lisboa 1649-003, Portugal*

(Received 21 January 2008; published 16 July 2008)

The dynamics of matter waves in linear and nonlinear optical lattices subject to a spatially uniform linear force is studied both analytically and numerically. It is shown that by properly designing the spatial dependence of the scattering length it is possible to induce long-living Bloch oscillations of gap-soliton matter waves in optical lattices. This occurs when the effective nonlinearity and the effective mass of the soliton have opposite signs for all values of the crystal momentum in the Brillouin zone. The results apply to all systems modeled by the periodic nonlinear Schrödinger equation, including propagation of light in photonic and photorefractive crystals with tilted band structures.

DOI: [10.1103/PhysRevLett.101.030405](https://doi.org/10.1103/PhysRevLett.101.030405)

PACS numbers: 03.75.Kk, 03.75.Lm, 67.85.Hj

A striking consequence of the theory of Bloch electrons in a perfect crystal [1] is the one concerning the dynamical localization of a charge particle in a uniform electric field, a phenomenon which has been known as Bloch oscillation (BO) [2]. Besides solid state physics, where the phenomenon has been observed only in recent times [3], it is possible to implement BO in nonlinear optics, using light beams in arrays of waveguides [4], laterally confined Bragg mirrors [5], microcavities [6], in photorefractive crystals [7], or in systems of either linear ultracold atoms [8] or Bose-Einstein condensates (BECs) [9] in optical lattices (OLs). Apart from its fundamental significance, the interest in BO arises mainly from perspectives of practical applications. In this context we mention the use of BO for metrological tasks, including precise definition of  $h/m$  [10] and measurement of forces at the micrometer scale such as the Casimir-Polder force [11] and gravity [12]. Recently, BO were also suggested as a tool for controlling light in coupled-resonator optical waveguides [13]. In all these diverse contexts BO have been observed mainly in the linear regimes. In most typical situations, however, the nonlinearity appears as an intrinsic feature of the system which cannot be eliminated without losing the phenomenon. In the case of BEC, for example, the nonlinearity induced by two-body interactions allows the enhancement of the wave function localization through the formation of gap solitons [14]. The enhancement of localization in turn permits us to increase the spatial resolution of the BO, a feature which could be very useful for high precision metrological tasks.

The fact that BO can exist in the presence of interactions was first recognized in the context of nonlinear discrete systems [15]. For periodic continuous models of the nonlinear Schrödinger (NLS) type, such as ones describing matter waves in OLs [16], the existence of BO becomes more problematic because of nonlinearity induced instabilities in the underlying linear system. These instabilities

can be simply understood by observing that in a usual OL at the edges of an allowed band the effective mass has always opposite signs. This implies that if a Bloch state is modulationally stable (in presence of a constant nonlinearity) at one edge of the band, it must be necessarily unstable at the other band edge [18]. Instabilities and enhanced dispersion have been extensively investigated both theoretically [18,19] and experimentally [20] and have been identified as the primary causes for the short lifetimes of BO of matter waves observed both in numerical [21] and in real experiments [20].

In this Letter we show for the first time that by properly designing the nonlinearity in a system it is possible to achieve *long-living* BO of nonlinear waves. We propose to control the existence and stability properties of gap solitons, which are responsible for the distortionless dynamics of wave packets, by means of a spatial periodic modulation of the scattering length  $a_s$  using optically induced Feshbach resonance [22] (alternatively, spatially inhomogeneous nonlinearity can be produced by a periodic magnetic field [23]). This modulation corresponds to a *nonlinear* OL whose amplitude, considered as a free parameter, can be used to change the stability properties of the Bloch states at the edges of the band. We show that the parameter regions for which Bloch states become unstable in the whole band coincide with those for which long-lived BO of matter waves become possible. A condition for this to occur is that the effective nonlinearity and the effective mass have opposite signs for all values of the wave vector in the Brillouin zone (BZ). We mention that periodically varying nonlinearities were also considered in nonlinear optics [24] for the sake of compensating phase mismatch in second harmonic generation. No use of this technique, however, has been suggested so far to overcome the problem of the decay of BO in a nonlinear regime. Although in this Letter we concentrate on long-living BO of BEC gap solitons, similar results apply also to gap solitons of pho-

tonic and photorefractive crystals with tilted band structures.

We start with the following normalized NLS equation

$$i\psi_t = -\psi_{xx} + \gamma x\psi + \mathcal{U}(x)\psi + \mathcal{G}(x)|\psi|^2\psi, \quad (1)$$

describing an array of BECs in linear and nonlinear  $\pi$ -periodic lattices of the form  $\mathcal{U}(x) = \mathcal{U}(-x) = \mathcal{U}(x + \pi)$  and  $\mathcal{G}(x) = \mathcal{G}(x + \pi)$ , respectively, and the external linear force  $\gamma$  arising from an uniform acceleration of the lattices. In Eq. (1) the spatial and temporal variables are measured in units of  $d/\pi$  and  $\hbar/E_R$ , respectively, while the energy is measured in units of the recoil energy  $E_R = \hbar^2 \pi^2 / (2md^2)$ , where  $d$  is the lattice period and  $m$  is the atomic mass. In the absence of nonlinearity,  $\mathcal{G}(x) = 0$ , we have the familiar framework of band theory, with the linear eigenvalue problem  $-d^2 \varphi_{nq} / dx^2 + \mathcal{U}(x) \varphi_{nq} = E_n(q) \varphi_{nq}$ , and Bloch function  $\varphi_{nq}$ ,  $n$  denoting the band index and  $q$  the wave vector inside the first BZ  $q \in [-1, 1]$ . The periodicity of the linear OL induces a band spectrum for which  $E_n(q)$  are periodic in the reciprocal space. The effect of the linear force on a Bloch wave packet is described by the semiclassical equations of motion

$$\dot{x} = v_n(q) = dE_n(q)/dq, \quad \dot{q} = -\gamma, \quad (2)$$

where  $x$  and  $q$  denote the wave packet centers in real and in reciprocal spaces, respectively,  $v_n(q)$  is the Bloch velocity, and the dot stands for the time derivative. From these equations it follows that, when transitions to other bands can be neglected, e.g. for small  $\gamma$ , the momentum distribution moves through  $q$ -space at a constant speed, while preserving its shape. In the real space the wave packet oscillates back and forth executing BO with spatial and temporal periods given by  $X_s = \Delta E_n / 2|\gamma|$  ( $\Delta E_n$  is the bandwidth) and  $T_s = 2/|\gamma|$ , respectively.

To understand the mechanism preventing the existence of BO in the nonlinear case, we concentrate on the lowest energy band (we will omit therefore the band index) and assume the linear force to be weak enough  $\gamma \ll 1$  [25]. Next we search for a localized solution of (1) in the form of a multiple scale expansion  $\psi = \gamma^{1/2} \psi_1 + \gamma \psi_2 + \dots$ , with  $\psi_j$  functions of the scaled temporal and spatial variables  $t_j = \gamma^{j/2} t$  and  $x_j = \gamma^{j/2} x$  ( $j = 1, 2, \dots$ ), respectively. As first order function we take  $\psi_1 = A(\tau, X) e^{i\mathcal{E}(t)} \varphi_{q(\tau)}(x)$  where  $A$  is the envelope depending on slow time  $\tau = \gamma t$  and on slow spatial variable  $X = \sqrt{\gamma}(x - v(\tau)t)$  with  $v$  exactly given by the Bloch velocity  $v(q)$ ,  $q$  is the carrier wave vector depending on  $\tau$ , and  $\mathcal{E}(t)$  is a phase determined by the equation  $d\mathcal{E}/dt = E(q(\gamma t))$ . By substituting the above ansatz into Eq. (1) and separating it into different orders of  $\gamma^{1/2}$ , we find that the equation of the first two orders are automatically satisfied (see, e.g., [18]). The nonlinearity appears at the third order of the expansion,  $\mathcal{O}(\gamma^{3/2})$ , where for eliminating secular terms one has to use Eqs. (2) [26]. Then the envelope  $A$  evolves

according to the NLS equation

$$iA_\tau + (2M(q))^{-1} A_{XX} - \chi(q)|A|^2 A = 0, \quad (3)$$

where  $M(q) = (d^2 E(q)/dq^2)^{-1}$  is the effective mass and  $\chi(q) = \int_{-\pi}^{\pi} \mathcal{G}(x) |\varphi_{q(\tau)}(x)|^4 dx$  the effective nonlinearity. From this we conclude that for gap solitons of Eq. (1) the semiclassical equations (2) continue to be valid also in the nonlinear case. Notice that although we have indicated  $q$  as an argument in the above definitions of  $M$ ,  $\chi$ , the group velocity, the effective mass and the effective nonlinearity are functions of the slow time  $\tau$ .

The existence of solitons of Eq. (3), however, is conditioned by the constrain  $M(q)\chi(q) < 0$ , this assuring instability of the Bloch state with  $q$ . Since at different band edges the effective mass has opposite signs, it is clear from the expression of  $\chi(q)$  that at a constant nonlinearity  $\mathcal{G}(x) = \text{const}$  stationary gap solitons can exist only at one of the edges (for which  $M\chi < 0$ ). This results in decay of BO simply because the wave packet moving according to (2) will necessarily reach the edge of the band where  $M\chi > 0$ , i.e., where the Bloch state becomes stable due to the change of sign of the effective mass. Thus, to achieve long-living BO one must require  $M(q)\chi(q) < 0$  for *all*  $q$  in the BZ, this assuring the conditions for existence of a soliton in the whole band. The above condition can be achieved by a proper design of the nonlinearity.

For all numerical results we fix the OLs in Eq. (1) to be of the most typical form:  $\mathcal{U}(x) = -V \cos(2x)$ , and  $\mathcal{G}(x) = g + G \cos(2x)$ , with  $V$ ,  $G$ , considered as free parameters and  $g$  fixed as in Fig. 1 (other numerical values give similar results). Denoting by  $\chi_{0,1}$  the effective nonlinearities at the

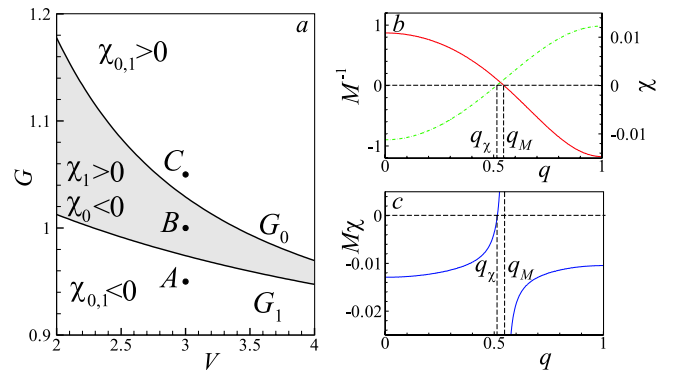


FIG. 1 (color online). (a) Curves  $G_{0,1}(V)$  separating domains where  $\chi_{0,1}(V) \geq 0$ , for  $g = -0.777$ . Points  $A$ ,  $B$ ,  $C$ , correspond to the parameters used in Fig. 2(b) (point  $A$ ), Figs. 2(a) and 3(a), (point  $B$ ), and Fig. 3(b) (point  $C$ ). Long-living BO exist for parameters inside the shadowed domain. (b) The inverse effective mass  $M^{-1}$  (solid line) and the effective nonlinearity  $\chi$  (dashed-dotted line) vs  $q$ , for the point  $B$  of panel (a). (c)  $M\chi$  vs  $q$  for parameters corresponding to point  $B$  in panel (a). Points  $q_M \approx 0.547$  and  $q_\chi \approx 0.514$  in panels (b),(c), denote the values of  $q$  where  $\chi$  and  $M^{-1}$  are, respectively, equal to zero.

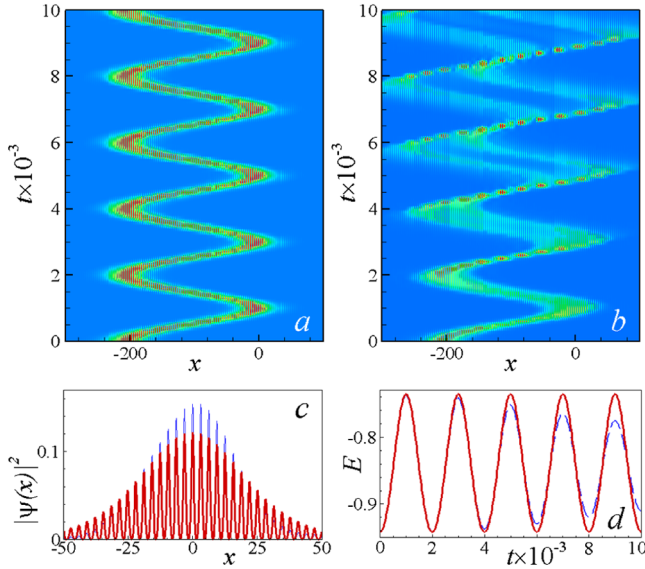


FIG. 2 (color online). Long-living (a) and decaying (b) BO for  $G = 1.0$  [point  $B$  in Fig. 1(a)] and  $G = 0.95$  [point  $A$  in Fig. 1(a)], respectively. In both cases the initial condition is a stationary gap-soliton located at  $X_0 = -65\pi$  with  $E = -0.938$  near the lower edge. Other parameters are  $\gamma = -0.001$  and  $V = 3.0$ . The period and the amplitude of the BO are  $T_s = 2 \cdot 10^3$  and  $X_s \approx 32.5\pi$  (for the  ${}^7\text{Li}$  condensate, mentioned in the text, these correspond to 45.2 ms and  $32.5 \mu\text{m}$ ). (c) The profile of the gap soliton in panel (a) at the fifth right turning point (thin lines) compared with the stationary state (thick lines) with the same  $N = 2.420$  ( $\approx 3800$  atoms in physical units) and energy  $E = -0.732$  close to the upper edge of the band. (d) Energy of the gap soliton vs time for long-living ( $G = 1.0$ , solid line) and decaying ( $G = 0.95$ , dashed line) BO. The lowest allowed band is  $E \in [-0.937, -0.733]$ .

edges of the band and by  $G_{0,1}$  the values of  $G$  at which  $\chi_{0,1}$  become zero (indexes “0”, “1” refer to  $q = 0, 1$ , respectively) we have that  $G \geq G_{0,1}$  implies  $\chi_{0,1} \geq 0$  and the condition  $M_{0,1}\chi_{0,1} < 0$  for the existence of gap-solitons at the both edges is satisfied if  $G_1 < G < G_0$  (the shadowed region of Fig. 1, e.g., in point  $B$ ). On the contrary, parameters above the  $G_0$  curve (e.g. point  $C$ ) or below the  $G_1$  curve (e.g., point  $A$ ) allow for the existence of gap solitons only at one of the edges (at the lower or the upper edge, respectively).

According to our analysis we should expect long-living BOs for amplitudes of the OLs corresponding to points between the two curves  $G_{0,1}(V)$  in Fig. 1. For the sake of definiteness we choose points  $A$ ,  $B$ , and  $C$  as shown in panel (a). Point  $B$  corresponds to almost an optimal design of the OLs as it is clear from panels (b) and (c) of Fig. 1. Note that while  $q_M$  and  $q_\chi$  are very close to each other, they do not exactly coincide, this giving a small interval  $q_\chi < q < q_M$  where envelope solitons do not exist. This region, however, being smaller than the spectral width of the soliton and very small compared to the size of the BZ, has no disruptive influence on the soliton dynamics. On the

contrary, points  $A$ ,  $C$ , in Fig. 1(a) correspond to the case in which the BO should quickly decay.

To check these predictions we have performed direct numerical integrations of Eq. (1). In Fig. 2(a) we show the time evolution of a gap soliton for parameters of the OLs corresponding to point  $B$  in Fig. 1. The existence of long-living BO, with temporal period and spatial amplitude perfectly matching the semiclassical estimates, is evident. The turning points of the spatial dynamics correspond to energies inside the gaps (close to band edges) for which stationary solitons exist. Comparing the shape of the stationary state at the top of the band with profiles of the dynamical solution at the right turning points, we find that they practically coincide [see Fig. 2(c)]. Also, the dynamical profiles of the soliton at all subsequent turning points are practically indistinguishable from the one depicted in Fig. 2(c). Numerical simulations performed on longer time scales (up to  $t = 2 \times 10^4$ ) showed no appreciable decay of the BO and perfect matching of the soliton shapes at the turning points. This behavior contrasts with the one observed in Fig. 2(b) where the dynamics of the soliton is shown for a non optimal design of the OLs (point  $A$  in Fig. 1): now BO undergo fast decay and the soliton quickly spreads out. The difference in the two types of BO becomes also evident by computing the soliton energy  $E(t) = \frac{1}{N} \int_{-\infty}^{\infty} (|\psi_x|^2 + \mathcal{U}(x)|\psi|^2 + \mathcal{G}(x)|\psi|^4) dx$ , with  $N = \int_{-\infty}^{\infty} |\psi|^2 dx$  denoting the soliton norm. This is shown in Fig. 2(d) from which we see that stable BO correspond to

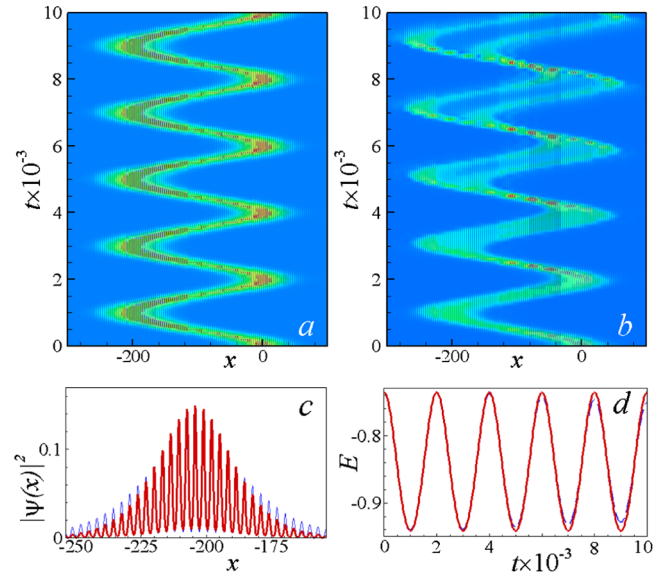


FIG. 3 (color online). Same as in Fig. 2 but with the BO started from a gap soliton near the top of the band at  $E = -0.732$ , with initial position  $X_0 = 0$ . Panels (a) and (b) refer, respectively, to points  $B$  and  $C$ , of Fig. 1, while panels (c) and (d) show corresponding quantities as in Fig. 2. In (c) we compare solitons at the fifth left turning point with the stationary state at  $E = -0.938$  near the lower edge, while in panel (d) the dashed line refers to  $G = 1.05$ .

perfectly periodic trajectory (solid line) while decaying BO correspond to decays of the oscillations of the energy (dashed line). Similar phenomena exist also if the BO is started from stationary states at the top of the band, with parameter values corresponding to points *B*, *C*, of Fig. 1(a) (see Fig. 3).

To discuss possible parameter designs for experimental implementations of the long-living BO we refer to a  $^7\text{Li}$  condensate in a trap of transverse size  $a_{\perp} = 2\mu\text{m}$  and with longitudinal linear and nonlinear OLs of the period  $d = 1\mu\text{m}$ . The dimensionless units of time, space, and energy in this case correspond to  $22.6\mu\text{s}$ ,  $318.3\text{nm}$ , and  $4.64 \times 10^{-30}\text{J}$ , respectively. The long-living BO dynamics depicted in Figs. 2(a) and 3(a), can be produced by an external force of  $1.45 \times 10^{-26}\text{N}$  (corresponding to an acceleration of the OLs of the order of  $\sim 1.24\text{m/s}^2$ ) acting on a gap soliton with about 3800 atoms, which is computed through the soliton norm  $N$  as  $(a_{\perp}^2 \pi / 4da_s)N$ . The nonlinear OL can be created by optically induced Feshbach resonance leading to a spatial variation of the scattering length of the form  $a_s(x) = a_s^{(0)} + a_s^{(1)} \cos(2\pi x/d)$ , with  $a_s^{(0)} = -1.554\text{nm}$  and  $a_s^{(1)} = 2\text{nm}$ . For the parameters of Fig. 1, the long-living BO then occur for an amplitude of the linear OL  $V = 3E_R$ , and a spatial variation of the scattering length in the range  $1.948\text{nm} < a_s^{(1)} < 2.058\text{nm}$ .

To conclude, we have shown how to achieve long-living BO in a system described by the NLS equation with periodic coefficients. This phenomenon occurs when the effective nonlinearity and the effective mass have opposite signs for all values of the wave vector, a condition which can be satisfied by properly modulating the nonlinearity in space. The results apply to numerous physical systems including matter waves, and photonic and photorefractive crystals.

M. S. acknowledges support from a No. MIUR-PRIN-2005 initiative. V. V. K. was supported by FCT and European program FEDER, Grant No. POCI/FIS/56237/2004. Y. V. B. acknowledges support from FCT, Grant No. SFRH/PD/20292/2004.

- 
- [1] F. Bloch, *Z. Phys.* **52**, 555 (1928).  
 [2] C. Zener, *Proc. R. Soc. A* **145**, 523 (1934).  
 [3] K. Leo, *Semicond. Sci. Technol.* **13**, 249 (1998).

- [4] U. Peschel, T. Pertsch, and F. Lederer, *Opt. Lett.* **23**, 1701 (1998).  
 [5] A. Kavokin *et al.*, *Phys. Rev. B* **61**, 4413 (2000).  
 [6] R. Sapienza *et al.*, *Phys. Rev. Lett.* **91**, 263902 (2003).  
 [7] H. Trompeter *et al.*, *Phys. Rev. Lett.* **96**, 053903 (2006).  
 [8] E. Peik *et al.*, *Phys. Rev. A* **55**, 2989 (1997); E. Peik *et al.*, *Appl. Phys. B* **65**, 685 (1997).  
 [9] D. I. Choi and Q. Niu, *Phys. Rev. Lett.* **82**, 2022 (1999); O. Morsch *et al.*, *Phys. Rev. Lett.* **87**, 140402 (2001); M. Cristiani *et al.*, *Phys. Rev. A* **65**, 063612 (2002); A. Kolovsky and H. Korsch, *Int. J. Mod. Phys. B* **18**, 1235 (2004).  
 [10] R. Battesti *et al.*, *Phys. Rev. Lett.* **92**, 253001 (2004); P. Cladé *et al.*, *Phys. Rev. A* **74**, 052109 (2006).  
 [11] I. Carusotto *et al.*, *Phys. Rev. Lett.* **95**, 093202 (2005).  
 [12] G. Ferrari, N. Poli, F. Sorrentino, and G. M. Tino, *Phys. Rev. Lett.* **97**, 060402 (2006).  
 [13] S. Longhi, *Phys. Rev. E* **75**, 026606 (2007).  
 [14] B. Eiermann *et al.*, *Phys. Rev. Lett.* **92**, 230401 (2004).  
 [15] R. Scharf and A. R. Bishop, *Phys. Rev. A* **43**, 6535 (1991); V. V. Konotop, O. A. Chubykalo, and L. Vázquez, *Phys. Rev. E* **48**, 563 (1993); D. Cai, A. R. Bishop, N. Grønbech-Jensen, and M. Salerno, *Phys. Rev. Lett.* **74**, 1186 (1995).  
 [16] Periodic one-dimensional models are applicable when  $a_s \ll a_{\perp} \ll \lambda \ll a_{\parallel}$ , where  $a_{\perp}$  and  $a_{\parallel}$  are the transverse and longitudinal trap lengths, and  $\lambda$  is the wave packet width (see, e.g., [17]).  
 [17] G. L. Alfimov, V. V. Konotop, and M. Salerno, *Europhys. Lett.* **58**, 7 (2002).  
 [18] V. V. Konotop and M. Salerno, *Phys. Rev. A* **65**, 021602 (2002).  
 [19] B. Wu and Q. Niu, *Phys. Rev. A* **64**, 061603 (2001); B. B. Baizakov, V. V. Konotop, and M. Salerno, *J. Phys. B* **35**, 5105 (2002); M. Machholm, C. J. Pethick, and H. Smith, *Phys. Rev. A* **67**, 053613 (2003); L. De Sarlo *et al.*, *Phys. Rev. A* **72**, 013603 (2005).  
 [20] L. Fallani *et al.*, *Phys. Rev. Lett.* **93**, 140406 (2004).  
 [21] R. G. Scott *et al.*, *Phys. Rev. Lett.* **90**, 110404 (2003); R. G. Scott *et al.*, *Phys. Rev. A* **69**, 033605 (2004).  
 [22] P. O. Fedichev, Yu. Kagan, G. V. Shlyapnikov, and J. T. M. Walraven, *Phys. Rev. Lett.* **77**, 2913 (1996).  
 [23] G. Dong and B. Hu, *Phys. Rev. A* **75**, 013625 (2007); F. Kh. Abdullaev, A. Abdumalikov, and R. Galimzyanov, *Phys. Lett. A* **367**, 149 (2007).  
 [24] V. Berger, *Phys. Rev. Lett.* **81**, 4136 (1998).  
 [25] Since the two-body interactions cannot give rise to particle transfer among bands, the condition  $\gamma \ll 1$  is enough to exclude the occurrence of Landau-Zener tunneling.  
 [26] The equation  $\dot{q} = -\gamma$  allows one to cancel the third order terms arising from the time dependence of  $q \equiv q(\gamma t)$ , using the identity  $-i \int_{-\pi}^{\pi} \bar{\varphi}_q \frac{\partial}{\partial q} \varphi_q dx = \int_{-\pi}^{\pi} x |\varphi_q|^2 dx$ .